Exploring the Oxygenase Function of Form II Rubisco for Production of Glycolate from CO2

Fan Yang
IMCAS: Institute of Microbiology Chinese Academy of Sciences https://orcid.org/0000-0001-5590-7951

Junli Zhang
Institute of Microbiology Chinese Academy of Sciences

Zhen Cai
Institute of Microbiology Chinese Academy of Sciences

Jie Zhou
Institute of Microbiology Chinese Academy of Sciences

Yin Li (yli@im.ac.cn)
Institute of Microbiology, Chinese Academy of Sciences

Original article

Keywords: Rubisco, oxygenase activity, glycolate production, cyanobacteria, CO2

Posted Date: February 24th, 2021

DOI: https://doi.org/10.21203/rs.3.rs-230143/v1

Abstract

The oxygenase activity of Ribulose-1,5-bisphosphate carboxylase/oxygenase (Rubisco) converts ribulose-1,5-bisphosphate (RuBP) into 2-phosphoglycolate, which in turn channels into photorespiration, resulting in carbon and energy loss in higher plants. We observed that glycolate can be accumulated extracellularly when two genes encoding the glycolate dehydrogenase of cyanobacteria *Synechocystis* sp. PCC 6803 were inactivated. This inspired us to explore the oxygenase function of Rubisco for production of glycolate, an important industrial chemical, from CO_2 by engineered cyanobacteria. Since the oxygenase activity of Rubisco is generally low in CO_2-rich carboxysome of cyanobacteria, we introduced Form II Rubisco, which cannot be assembled in carboxysome, into the cytoplasm of cyanobacteria. Heterologous expression of a Form II Rubisco from endosymbiont of tubeworm *Riftia pachyptila* (RPE Rubisco) significantly increased glycolate production. We show that the RPE Rubisco is expressed in the cytoplasm. Glycolate production increased upon addition of $NaHCO_3$ but decreased upon supplying CO_2. The titer of glycolate reached 2.8 g/L in 18 days, a 14-fold increase compared with the initial strain with glycolate dehydrogenase inactivated. This is also the highest glycolate titer biotechnologically produced from CO_2 ever reported. Photosynthetic production of glycolate demonstrated the oxygenase activity of Form II Rubisco can be explored for production of chemicals from CO_2.

Introduction

Ribulose-1,5-bisphosphate carboxylase/oxygenase (Rubisco) is the key enzyme in photosynthesis (Jensen RG 2000, Erb TJ and Zarzycki J 2018). It is responsible for the primary carbon fixation in Calvin-Benson-Bassham (CBB) cycle, catalyzing the addition of CO_2 to ribulose-1,5-bisphosphate (RuBP), leading to the formation of 3-phosphoglycerate (3PGA) (Moroney JV et al. 2013). Despite its pivotal role in the biosphere, Rubisco is notorious for its poor carboxylation activity and specificity (Davidi D et al. 2020). The poor specificity of Rubisco is due to its oxygenase activity, as CO_2 and O_2 are competitive substrates of Rubisco (Moroney JV, Jungnick N et al. 2013). The oxygenation reaction catalyzed by the oxygenase activity of Rubisco results in the production of 2-phosphoglycolate (2PG) (Eisenhut M et al. 2008). Although 2PG can be metabolized through photorespiration and recycled back into the central carbon metabolism, this process is energy-consuming and leads to carbon loss (Moroney JV, Jungnick N et al. 2013, Fernie AR and Bauwe H 2020).

The oxygenase activity of Rubisco is often considered undesirable but unavoidable (Moroney JV, Jungnick N et al. 2013). A compelling evidence is that active photorespiration is found in nearly all oxygenic photosynthetic organisms to metabolize 2PG, the toxic oxygenation product of Rubisco (Moroney JV, Jungnick N et al. 2013). Engineering Rubisco for a great carboxylation efficiency often comes at a price of decreased CO_2:O_2 specificity, not to mention the complete removal of its oxygenase activity (Davidi D, Shamshoum M et al. 2020). In fact, there are no CO_2 or O_2 binding sites found in Rubisco (Moroney JV, Jungnick N et al. 2013). Rubisco binds RuBP and converts it to the 2,3-enediol

form, allowing the subsequent addition of either CO_2 or O_2 (Spreitzer RJ and Salvucci ME 2002). Due to this catalytic mechanism of Rubisco, it is proposed that the oxygenation reaction of Rubisco cannot be eliminated by mutation (Moroney JV, Jungnick N et al. 2013).

Since the oxygenation function of Rubisco cannot be avoided, and the oxygenation product is involved in the overall carbon metabolism, we propose we can take this advantage to employ the oxygenase activity of Rubisco to produce useful chemicals. In *Synechocystis* sp. PCC 6803 (hereafter *Synechocystis*), 2PG is subsequently converted to glycolate, a versatile chemical with a wide range of industrial applications in cosmetics, pharmaceuticals and biodegradable polymeric material production (Eisenhut M et al. 2006, Eisenhut M et al. 2008, Zahoor A et al. 2014, Zhan T et al. 2020). Thus, we intended to produce glycolate from CO_2 using the oxygenase activity of Rubisco in *Synechocystis*, providing a unique application avenue of the oxygenase activity in photosynthetic biosynthesis.

Methods And Material

Plasmids and strains construction

All plasmids constructed in this study were summarized in Supplemental Table 1. *Escherichia coli* DH5a was used as the host for plasmids construction. All plasmids were generated through Gibson Assembly (NEB, China) of amplified inserts and linearized pUC57 plasmid backbones with primers designed using NEBuilder Assembly Tool (http://nebuilder.neb.com/). All *Synechocystis* mutant strains constructed in this study were summarized in Supplemental Table 1. Cyanobacterial strains were generated by transforming cells with certain plasmids which included homologous regions as well as the inserts. Rubiscos were individually overexpressed under the control of the promoter P_{cpc560}. The DNA cassette together with a chloromycetin resistance marker was integrated into *pta* site of *Synechocystis* genome. Transformation of *Synechocystis* was performed as previously described (Lindberg P et al. 2010). The colonies were selected on BG-11 plates supplemented with single or combined antibiotics (10 μg/mL chloromycetin, 30 μg/mL erythromycin, 10 μg/mL spectinomycine). Complete segregation and correct gene insertions were checked by PCR and sequencing with primers listed in Supplemental Table 2.

Culture conditions

All strains were grown in 50 mL erlenmeyer flask containing 20 mL of BG11 medium at 30^oC under a constant illumination intensity of 100 μmol photons $m^{-2}s^{-1}$, with atmospheric CO_2 level or supplemented with prescribed concentration of $NaHCO_3$. The initial OD_{730} was normalized to 0.5. Antibiotics were added to the culture for routine maintenance of mutants when necessary. Growth was monitored by measurements of the optical density at 730 nm (OD_{730}) every three days.

Quantification of extracellular glycolate concentration

Extracellular glycolate concentrations were determined using the culture supernatants every three days. 10 µL of culture supernatant was analyzed by HPLC equipped with Bio-Rad Aminex® HPX-87H Ion Exclusion Column (300 mm × 7.8 mm) using 8 mM H_2SO_4 as mobile phase, pumped at a flow rate of 0.6 ml/min. The column temperature was maintained at 50°C, peaks were detected using Agilent Technologies 1260 RID (refractive index detector).

Quantification of intracellular 2PG and glycolate concentration

The intracellular concentration of 2PG and glycolate were determined after three days of cultivation. To rapidly quench the cell metabolism, 5 mL of cultures were cooled to 0^{o}C within 15 s in a -50^{o}C methanol bath. After centrifugation at 4^{o}C for 5 min at 8,000 g, the cell pellets were washed once with precooled water and resuspended in 2 mL of precooled 80% (vol/vol) methanol solution. After incubation at -20^{o}C for 30 min, the samples were then centrifuged at 4^{o}C for 10 min at 20,000 g. The supernatants were dried by lyophilization and redissolved in 200 µL of water.

The concentration of 2PG and glycolate was determined with AB Sciex Qtrap 6500 LC-MS/MS System. Injection volume was 5 µL. Metabolites were separated with a HyperREZ XP Organic acid column (100 × 7.7 mm, Thermo Fisher Scientific) with H_2O as the solvent. The column was maintained at 40^{o}C with a solvent flow rate of 0.4 mL min^{-1}. The electrospray ionization MS was operated in the negative ion mode. The mass spectra were acquired in multiple-reaction monitoring model for the optimized ion pairs of 2PG and glycolate.

Enzyme assay

To prepare the protein samples for SDS PAGE and Native PAGE, *Synechocystis* cells were harvested by centrifugation and resuspended with 1 mL buffer (50 mM Tris-HCl, pH 8.0, 10 mM $MgCl_2$, 1 mM EDTA) for ultrasonication. After centrifugation, the supernatants were mixed with SDS loading buffer or Native loading buffer at 1:1. The protein samples were detected with SDS PAGE or Native PAGE after the total protein amount was normalized to 7 µg.

Fluorescence microscopy

5 µL log-phase cells were spotted onto 1% (w/v in BG11) agarose pads and air-dried before application of a 0.17 mm coverglass. Fluorescence microscopy was performed on a Nikon N-SIM-S Super Resolution Microscope with a 63x/1.4 NA oil-immersion objective using laser lines at 488, and 561 nm.

Results

Inactivation of two genes encoding glycolate dehydrogenase in Synechocystis resulted in glycolate production

In *Synechocystis*, glycolate is converted to glyoxylate by two glycolate dehydrogenases (GlcD1 and GlcD2), and subsequently metabolized by three branched routes (Eisenhut M, Kahlon S et al. 2006, Eisenhut M, Ruth W et al. 2008). To completely block the glycolate metabolism, both GlcD1 and GlcD2 encoded by *glcD1* and *glcD2*, respectively, were inactivated (Fig. 1). The resulting mutant was designated as WT-ΔglcD (Table 1). Complete segregation and correct gene insertions at both *glcD1* and *glcD2* sites were verified by PCR and sequencing (Fig. S1).

Table 1
The Synechocystis strains used in this study

Strain	Genetic background	Source of Rubisco
Wild type	*Synechocystis* sp. PCC 6803	-
WT-ΔglcD	WT Δ*glcD1*::*em*^{r}; Δ*glcD2*::*spec*^{r}	-
RPE-ΔglcD	Δ*glcD* Δ*pta*::P_{cpc560}-*rpe*-T_{rbcs}-*cm*^{r}	*Riftia pachyptila* endosymbiont
4Pm-ΔglcD	Δ*glcD* Δ*pta*::P_{cpc560}-*4pm*-T_{rbcs}-*cm*^{r}	*Phaeospirillum molischianum*
5St-ΔglcD	Δ*glcD* Δ*pta*::P_{cpc560}-*5st*-T_{rbcs}-*cm*^{r}	*Sedimenticola thiotaurini*
6RBC-ΔglcD	Δ*glcD* Δ*pta*::P_{cpc560}-*6rbcL-6rbcS*-T_{rbcs}-*cm*^{r}	*Synechocystis* sp. PCC 6803

As glycolate metabolism was completely blocked, we next investigated glycolate accumulation in strain WT-ΔglcD. Both the intracellular and extracellular glycolate concentration of WT-ΔglcD were analyzed and compared with that of the WT strain. Samples were taken after three days cultivation supplemented with or without 50 mM $NaHCO_3$. The intracellular glycolate concentration of the WT strain was 0.004 μmol $L^{-1}OD_{730}{}^{-1}$ and 0.02 μmol $L^{-1}OD_{730}{}^{-1}$ respectively, when supplemented with or without 50 mM $NaHCO_3$ (Fig. S2). Moreover, the extracellular glycolate concentration was undetectable in the WT strain under both conditions (data not shown). It is evident that glycolate could be rapidly metabolized in the WT strain. On the contrary, strain WT-ΔglcD accumulated glycolate intracellularly and extracellularly under both conditions (Fig. 2 and Fig. S2). The intracellular glycolate concentration of strain WT-ΔglcD was 0.51 μmol $L^{-1}OD_{730}{}^{-1}$ when supplied with 50 mM $NaHCO_3$, and increased to 1.75 μmol $L^{-1}OD_{730}{}^{-1}$ without the supply of $NaHCO_3$ (Fig. S2). Furthermore, the glycolate concentration in the medium of strain WT-ΔglcD reached 86.47 μmol $L^{-1}OD_{730}{}^{-1}$ (mass concentration of 0.02 g/L) and 317.77 μmol $L^{-1}OD_{730}{}^{-1}$ (mass concentration of 0.06 g/L) after 3 days cultivation respectively, with or without 50 mM $NaHCO_3$ (Fig. 2). Apparently, the majority of glycolate was excreted to the culture by strain WT-ΔglcD, and the intercellular glycolate accumulation could be negligible. We further monitored the glycolate concentration

in the medium every three days and found that strain WT-ΔglcD produced 0.19 g/L and 0.34 g/L of glycolate after 18 days cultivation respectively with or without the supply of 50 mM $NaHCO_3$ (Fig. 2). In other words, glycolate can be produced from CO_2 and secreted extracellularly upon inactivation of the two glycolate dehydrogenases in *Synechocystis*. Moreover, strain WT-ΔglcD produces higher concentration of glycolate when no additional $NaHCO_3$ was supplemented, suggesting ambient level CO_2 is sufficient for glycolate production to occur.

Overexpression of the native carboxysome-located Rubisco does not contribute to glycolate production

Given the multiple industrial applications of glycolate, we were encouraged to further increase glycolate production. Glycolate synthetic pathway comprises two reactions (Fig. 1). RuBP reacts with O_2 to generate one molecule of 2PG and one molecule of 3-Phosphoglycerate (3PGA) (Eisenhut M, Ruth W et al. 2008, Fernie AR and Bauwe H 2020). 2PG is then dephosphorylated to glycolate and 3PGA enters the CBB cycle to regenerate RuBP (Eisenhut M, Ruth W et al. 2008, Fernie AR and Bauwe H 2020). In order to identify the bottleneck of glycolate production, the intercellular 2PG concentration in the WT strain and strain WT-ΔglcD were measured. Samples were taken after three days cultivation with or without the supply of 50 mM $NaHCO_3$. With the intact glycolate metabolism, the intracellular 2PG concentration in the WT strain were below 0.03 μmol $L^{-1}OD_{730}{}^{-1}$ under both growth conditions (Fig. S2). The intracellular 2PG level in strain WT-ΔglcD was at the same level as compared to the WT strain. However, as mentioned above, the intracellular glycolate concentration in strain WT-ΔglcD became about 100-fold higher than that of the WT strain irrespective of the supply of 50 mM $NaHCO_3$ (Fig. S2). This indicated that the conversion from 2PG to glycolate in strain WT-ΔglcD was efficient and that the oxygenation of RuBP catalyzed by Rubisco was the rate-limiting step of glycolate production.

Thus, to increase glycolate production, the native Rubisco of *Synechocystis* was overexpressed in strain WT-ΔglcD. The resulting mutant was designated as strain 6RBC-ΔglcD (Table 1) and its capacity for glycolate production was determined with the same growth conditions as mentioned above. After 18 days of cultivation, strain 6RBC-ΔglcD produced 0.16 g/L and 0.35 g/L of glycolate when supplied with or without 50 mM $NaHCO_3$, respectively. Neither titer is significantly higher than that of strain WT-ΔglcD under the same condition (Fig. 3a and b). In addition, no significant difference was observed in the growth rate of strains 6RBC-ΔglcD and WT-ΔglcD under both conditions (Fig. 3c and 3d). Moreover, the SDS PAGE and native PAGE results suggested that 6RBC was successfully overexpressed and assembled under both conditions (Fig. 3e and f). These results together suggested that overexpression of 6RBC Rubisco did not contribute to increase glycolate production. The reason behind is likely that the native 6RBC Rubisco is encapsulated in a microcompartment found in all cyanobacteria, termed as the carboxysome. It reduces the oxygenase activity of Rubisco by inhibiting the entrance of O_2 and increasing CO_2 concentration around Rubisco (Espie GS and Kimber MS 2011). Thus, to increase

glycolate production, the selected Rubisco is expected to be located outside the carboxysome so as its oxygenase activity can play a role.

Overexpression of Form II Rubiscos enhanced glycolate production

It was previously reported that replacing the native Rubisco of cyanobacteria with Form II Rubisco could not support the biogenesis of carboxysome, indicating the Form II Rubisco resides outside the carboxysome (Baker SH et al. 1998, Durao P et al. 2015). If the Rubisco is located in the cytosol, it is accessible to molecule oxygen and a reduced CO_2 level due to the absence of carbonic anhydrase in the cytosol (Price GD et al. 2008, Price GD 2011). Thus, we hypothesized that Form II Rubiscos might be promising candidates to increase glycolate production. To this end, three form II Rubiscos from *Riftia pachyptila* endosymbiont (RPE Rubisco), *Phaeospirillum molischianum* (4Pm Rubisco) and *Sedimenticola thiotaurini* (5St Rubisco) were selected and individually overexpressed by using the strong promoter P_{cpc560} in strain WT-ΔglcD (Table 1), resulting in strains RPE-ΔglcD, 4Pm-ΔglcD and 5St-ΔglcD, respectively (Fig. S1).

Subsequently, glycolate production of these three strains were determined without additional $NaHCO_3$, which seemed to be more favorable for strain WT-ΔglcD to produce glycolate. After 18 days of cultivation, strain 5St-ΔglcD produced 0.3 g/L glycolate, which is not significantly higher than that of strain WT-ΔglcD (Fig. 3a). Moreover, no significant difference on growth were observed between them (Fig. 3c). This incapacity for increasing glycolate production could be attributed to the undetectable expression and assembly of 5St Rubisco (Fig. 3e). In contrast, glycolate production was dramatically enhanced in strains RPE-ΔglcD and 4Pm-ΔglcD (Fig. 3a). After 18 days cultivation, strain 4Pm-ΔglcD produced 0.66 g/L of glycolate, about twofold of strain WT-ΔglcD, while strain RPE-ΔglcD produced 0.87 g/L of glycolate, 2.6-fold of strain WT-ΔglcD (Fig. 3a). However, the growth of strains RPE-ΔglcD and 4Pm-ΔglcD were significantly impaired (Fig. 3c). The expression and assembly of RPE Rubisco and 4Pm Rubisco were also detected (Fig. 3e). RPE Rubisco was copiously overexpressed and well assembled. By contrast, 4Pm Rubisco was successfully overexpressed but not assembled well. This explained their different capacity on enhancement of glycolate production. Taken together, these results showed that overexpression of Form II Rubisco indeed increased glycolate production.

Supply of $NaHCO_3$ increased glycolate production by strains RPE-ΔglcD and 4Pm-ΔglcD

As mentioned above, glycolate production by strain WT-ΔglcD decreased when supplied with 50 mM $NaHCO_3$ (Fig. 2). Thus, we further investigated whether glycolate production of strains RPE-ΔglcD and 4Pm-ΔglcD would also be repressed when supplied with 50 mM $NaHCO_3$.

Surprisingly, glycolate production by strains RPE-ΔglcD and 4Pm-ΔglcD was not decreased, but instead sharply when $NaHCO_3$ was available (Fig. 3b). Strain 4Pm-ΔglcD produced 1.46 g/L of glycolate in 18 days when supplemented with 50 mM $NaHCO_3$, which is about 7.7-fold of the titer of strain WT-ΔglcD under the same condition (Fig. 3b). This is also more than twofold of the titer produced by Strain 4Pm-ΔglcD without additional $NaHCO_3$. Additionally, 4Pm Rubisco assembled better in strain 4Pm-ΔglcD upon addition of 50 mM $NaHCO_3$, which could contribute to the increased glycolate production (Fig. 3f). Among these three strains, strain RPE-ΔglcD was inarguably the best glycolate producer, generating 2.82 g/L after 18 days of cultivation, about 15-fold of the titer of strain WT-ΔglcD under the same growth condition (Fig. 3b). Moreover, the expression and assembly of RPE did not differ upon addition of $NaHCO_3$ (Fig. 3f), suggesting that the increased glycolate production was not related to the assembly of RPE Rubisco. However, the growth of strains RPE-ΔglcD and 4Pm-ΔglcD were also significantly impaired under this condition (Fig. 3d)

Thus, we further investigated glycolate production of strain RPE-ΔglcD when supplied with different concentration of $NaHCO_3$. Glycolate production of strain RPE-ΔglcD increased along with increasing the concentration of $NaHCO_3$, and approached a plateau of 2.84 g/L when supplied with 30 mM $NaHCO_3$ (Fig. 4a). Notably, the growth of strain RPE-ΔglcD gradually reduced along with the increased glycolate production (Fig. 4b). The intracellular glycolate concentration in RPE-ΔglcD was also increased, from 5.6 μmol $L^{-1}OD_{730}^{-1}$ in the absence of $NaHCO_3$, to 10.4 μmol $L^{-1}OD_{730}^{-1}$ when adding 50 mM $NaHCO_3$ (Fig. S2). It was previously reported that intracellular accumulation of glycolate is toxic to the cell (Eisenhut M, Ruth W et al. 2008). The retarded growth of strain RPC-ΔglcD upon adding increased concentration of $NaHCO_3$ was probably related to the elevated intracellular glycolate concentration in strain RPE-ΔglcD.

Supply of CO_2 decreased glycolate production by strain RPE-ΔglcD.

Cyanobacteria can use both HCO_3^- and CO_2 as external inorganic carbon source (Price GD, Badger MR et al. 2008, Price GD 2011). As supply of HCO_3^- increased glycolate production of strains RPE-ΔglcD and 4Pm-ΔglcD, we then wondered what would be the effect if supplying CO_2. Since strain RPE-ΔglcD produces much higher glycolate concentration than that of strain 4Pm-ΔglcD, we chose strain RPE-ΔglcD to study the effect of CO_2.

To this end, the external organic carbon supplied was changed from $NaHCO_3$ to CO_2. The glycolate production and growth of strain RPE-ΔglcD were evaluated under 1% or 3% CO_2 (Fig. 4c and 4d). After 12 days of cultivation, strain RPE-ΔglcD produced 0.87 g/L glycolate under 1% CO_2, and the glycolate titer decreased to 0.47 g/L under 3% CO_2 (Fig.4c). Additionally, the growth of strain RPE-ΔglcD increased positively with increasing the CO_2 level (Fig. 4d). The increased growth and reduced glycolate production

of RPE-ΔglcD together indicated that supply of CO_2 enhanced the carboxylation reaction of RPE and consequently inhibited the oxygenation reaction.

RPE Rubisco is located in the cytosol

The enhanced glycolate production indicated an active oxygenation reaction catalyzed by RPE Rubisco and 4Pm Rubisco. This suggested that they are probably located in the cytosol rather than in the carboxysome as the O_2 concentration in cytosol is much higher. To provide direct evidence, we visualized their location *in vivo* by fluorescent labelling. We first tried to carry out the co-localization analysis by labelling RPE Rubisco with cyan fluorescent protein (CFP) and 6RBC with yellow florescent protein (YFP). RPE Rubisco was labelled with CFP at its C-terminal (termed as RPE-CFP). YFP was fused to the C-terminal of the large subunit of 6RBC (termed as 6RBCL-YFP). RPE-CFP and 6RBCL-YFP were individually expressed in the WT strain to give single fluorescent signal and co-expressed in the WT-strain to test whether these two fluorescent signals could be overlayed together. However, the fluorescent signals of RPF-CFP and 6RBCL-YFP were too week to give the location information (data not shown).

We next fused green fluorescent protein (GFP) to the C-terminal of RPE Rubisco or the large subunit of 6RBC Rubisco, termed as RPE-GFP and 6RBCL-GFP, respectively. RPE-GFP and 6RCBL-GFP were individually expressed in the WT strain to give single fluorescent signal. Meanwhile, the red fluorescence of endogenous chlorophyll-a of *Synechocystis* was used to indicate the shape of the whole cell (Cameron J et al. 2013). RPE-GFP gave rise to a large single fluorescent punctum at the cell polar, suggesting that RPE proteins intended to aggregate at the edge of cell (Fig. 5a). By contrast, 6RBCL-GFP intended to exhibit several fluorescent spots at a more central position within the cell, indicating the location of mature carboxysomes, which was in agreement with the previous report (Fig. 5b) (Cameron J, Wilson S et al. 2013). The different position of fluorescent signals between RPE-GFP and 6RBC-GFP indicated that RPE is not located in the carboxysome where 6RBC-GFP resides. The bacterial Form II Rubisco from *Rhodospirillum rubrum* was previously expressed in the Δrbc strain of *Synechocystis* (Durao P, Aigner H et al. 2015). The resulting mutant could not support the biogenesis of carboxysome and photoautotrophic growth at ambient CO_2 concentration (Durao P, Aigner H et al. 2015). Thus, it is conceivable that the aggregate of RPE-CFP observed here is most likely in the cytosol.

Discussion

The oxygenase function of Rubisco and the ensuing photorespiration have long been regarded as one of the obstacles to improve the photosynthesis efficiency (South PF et al. 2018, Hu GP et al. 2019, Luan GD et al. 2020). Cumulative studies have attempted to inhibit even avoid the occurrence of the oxygenation reaction of Rubisco but gained limited progress (Erb TJ and Zarzycki J 2018, Davidi D, Shamshoum M et al. 2020). Here, as the oxygenation product of Rubisco is involved in the overall carbon metabolism, we utilized the oxygenation activity of Form II Rubisco for production of glycolate, a versatile chemical with extensive industrial applications, from CO_2 in *Synechocystis*.

In *Synechocystis*, glycolate can only be generated from 2PG, the direct product of the oxygenation reaction of Rubisco. Glycolate is then converted to glyoxylate and subsequently metabolized by three branched routes including the plant-like photorespiratory cycle, the bacterial glycerate pathway and the complete decarboxylation of glyoxylate to CO_2 (Eisenhut M, Ruth W et al. 2008). In the first instance, glycolate production was primarily achieved by inactivation of two forms of glycolate dehydrogenases which are responsible for converting glycolate to glyoxylate. As glycolate metabolism is completely inactivated, the resulting strain WT-ΔglcD produced glycolate irrespective of the provision of $NaHCO_3$. This indicated that Rubisco is performing the oxygenase reaction despite the active CO_2-concentrating mechanism (CCM) in carboxysome and the abundance of inorganic carbon, which is also proved in the earlier studies (Eisenhut M, Kahlon S et al. 2006, Eisenhut M, Ruth W et al. 2008). It is still under discussion whether cytosolic Rubisco, which is in the various stages of assembly during carboxysome biogenesis, is responsible for this oxygenase activity, or whether significant amounts of O_2 indeed enter the carboxysome (Espie GS and Kimber MS 2011, Burnap RL et al. 2015). Since overexpression of 6RBC Rubisco showed no effect on glycolate production, it is conceivable that the availability of O_2 is limited in carboxysome.

Additionally, inactivation of glycolate metabolism was reported to render a High CO_2 Requiring (HCR) phenotype which means the mutant was not able to grow at ambient CO_2 level (Eisenhut M, Ruth W et al. 2008). This HCR phenotype was presumably ascribed to the intracellular accumulation of toxic amounts of glycolate (Eisenhut M, Ruth W et al. 2008). It was reported that the intracellular glycolate concentration in the mutant increased to a much higher level within a few hours after the mutant was transferred from HC (5% CO_2) to LC (air, 0.035% CO_2) condition (Eisenhut M, Ruth W et al. 2008). Interestingly, strain WT-ΔglcD that we constructed did not exhibit the HCR phenotype (Fig. S3). Further investigation suggested that strain WT-ΔglcD did accumulate intracellular glycolate, but more than 99% of glycolate was excreted to the culture (Fig. 2 and Fig. S2). Glycolate excretion was previously observed in some filamentous cyanobacterial strains but not in *Synechocystis*, nor in mutant with HCR phenotype (Eisenhut M, Kahlon S et al. 2006, Eisenhut M, Ruth W et al. 2008). It is likely that glycolate excretion of strain WT-ΔglcD helped maintain the intracellular glycolate concentration at a low level, which allows the cell to grow normally at ambient CO_2 level, without displaying the HCR phenotype.

To further increase glycolate production, we identified the rate-limiting step by measuring the intracellular 2PG and glycolate concentrations of strain WT-ΔglcD. The result indicated that the conversion from 2PG to glycolate is fully active. As such, the oxygenase activity of Rubisco is the bottleneck of glycolate production, thus its activity needs to be increased. Accessibility to molecular oxygen is the prerequisite for the oxygenation reaction of Rubisco to occur. Overexpression of the native carboxysome-located 6RBC Rubisco of *Synechocystis* in strain WT-ΔglcD did not increase glycolate production, indicating that the oxygenation reaction of 6RBC Rubisco is hampered in the carboxysome which is a CO_2-rich but O_2-sheilding microcompartment (Price GD, Badger MR et al. 2008, Espie GS and Kimber MS 2011, Price GD 2011).

As compared to the carboxysome, the CO_2 concentration in the cytosol is much lower. To provide the gradient for inward diffusion of CO_2 and minimize its leakage from cell, cyanobacteria accumulate HCO_3^- but not CO_2 in the cytosol and maintained a chemical equilibrium in favor of HCO_3^- over CO_2 (Price GD, Badger MR et al. 2008, Price GD 2011, Burnap RL, Hagemann M et al. 2015). Thus, the low-CO_2-level cytosol might be a more favorable environment for the oxygenation reaction of Rubisco to occur. Additionally, as cyanobacteria perform oxygenic photosynthesis (Moroney JV, Jungnick N et al. 2013), the photosynthetic evolved O_2 from photosystem II located at the thylakoid membrane may also contribute to the glycolate production. Overexpression of an exogenous Form II Rubisco located in the cytosol indeed increased glycolate production. Among the three forms of Rubisco, there are three reasons why we consider Form II Rubiscos are promising candidates for glycolate production. First, the specificity of Form II Rubisco was reported to be extremely low, and thus can catalyze the oxygenation reaction more easily (Davidi D, Shamshoum M et al. 2020). Second, Form II Rubisco is not packaged in the carboxysome, as they do not support the carboxysome biogenesis (Baker SH, Jin S et al. 1998, Durao P, Aigner H et al. 2015). Third, Form II Rubiscos are structurally simple, comprising only a large subunit and commonly forming an L_2 or L_6 oligomer (Davidi D, Shamshoum M et al. 2020).

In this study, three form II Rubiscos were selected and individually overexpressed in strain WT-ΔglcD. Among them, both RPE Rubisco and 4Pm Rubisco increased glycolate production irrespective of carbon supplement. Strain RPE-ΔglcD produced the highest glycolate titer 2.8 g/L after 18 days of cultivation when supplied with 50 mM $NaHCO_3$ (Fig. 3b). Remarkably, it compares favorably over the majority of products synthesized from CO_2 in cyanobacteria (Oliver JWK and Atsumi S 2014, Gao XY et al. 2016). This indicated that the deceptively wasteful and undesired oxygenase activity of Rubisco has immense yet undeveloped ability with regard to photosynthetic bioproduction application.

It is interesting that supply of $NaHCO_3$ and CO_2 exhibits different effects on glycolate production by strain RPE-ΔglcD, as $NaHCO_3$ supply increased glycolate production while CO_2 supply decreased glycolate production. This could be related to the different manner of HCO_3^- and CO_2 entering the cell and the CCM applied by cyanobacteria. HCO_3^- is transported into the cytosol by the transporters located at the cytoplasmic membrane. The majority then enters the carboxysome and the sequestered carbonic anhydrase (CA) converts it to CO_2. RuBP enters the carboxysome and react with CO_2 catalyzed by the native Rubisco, generating two molecules of 3PGA. 3PGA escapes from the carboxysome and regenerate RuBP in the cytosol via CBB cycle (Fig. 6a). When supplied with $NaHCO_3$, the increased HCO_3^- availability generally facilitates the carbon fixation of the native Rubisco in the carboxysome and results in the enhanced of RuBP regeneration via CBB cycle (Fig. 6a). As regenerated in the cytosol, RuBP is preferentially oxygenated by RPE. Accordingly, less RuBP is channeled to biomass production, the growth of strain RPE-ΔglcD is impaired upon supplementation of additional $NaHCO_3$.

Furthermore, due to the absence of CA in the cytosol, the spontaneous conversion of HCO_3^- to CO_2 in the cytosol is much slower than the diffusion of CO_2 across the cytoplasmic membrane (Mangan NM et al.

2016). This means that supply of $NaHCO_3$ could not sharply raise the CO_2 concentration in the cytosol. The RPE Rubisco is identified from the chemolithoautotrophic symbiont in the trophosome of giant tubeworm *R. pachyptila* living at the deep-sea hydrothermal vents where the partial pressure of CO_2 can reach up to 2.9 kPa (Lutz RA et al. 1994). The internal total CO_2 concentration of *R. pachyptila* can approach up to 31 mM relying on the high concentration of CA in the worm's plume and trophosome tissue (Childress JJ et al. 1993). Therefore, it is possible that RPE Rubisco exhibits relatively low affinity to CO_2. Thus, the oxygenase activity of RPE is not inhibited even when supplied with 50 mM $NaHCO_3$.

As an uncharged small molecule, CO_2 can cross the cell membrane by diffusion (Price GD, Badger MR et al. 2008, Price GD 2011). Meanwhile, RPE Rubisco was not scattered inside the cell but aggregated near the cytoplasmic membrane. When supplied with CO_2, the relative concentration of CO_2 around RPE Rubisco is raised (as O_2 concentration is not changed) (Fig. 6b). Thus, oxygenation is inhibited and carboxylation is enhanced alone with the increased availability of CO_2. As a consequence, more RuBP is channeled to carbon fixation via CBB cycle, leading to increased cell growth and decreased glycolate production of strain RPE-ΔglcD when supplied with CO_2 (Fig. 6b).

In summary, we demonstrated that the oxygenase function of Form II Rubisco could be explored for production of chemicals, e.g. glycolate, from CO_2. Blocking the metabolism of photorespiration pathway led to glycolate production, and the efficiency for producing glycolate can be significantly improved when expressing Form II Rubisco in the cytosol. Thus, the Form II Rubisco with distinct peculiarity can exert their versatile extraordinary capability in photosynthetic biosynthesis applications.

Declarations

Authors’ contributions

Y.L. and J.Z. designed the research. F.Y., J.L.Z., C.Z. performed the research. Y.L. and F.Y. wrote the manuscript. All authors read and approved the manuscript.

Funding

This work was supported by Natural Science Foundation of China (31470231).

Ethics approval and consent to participate

Not applicable

Consent for publication

Not applicable

Acknowledgements

Not applicable

Authors' information

[1]CAS Key Laboratory of Microbial Physiological and Metabolic Engineering, State Key Laboratory of Microbial Resources, Institute of Microbiology, Chinese Academy of Sciences, Beijing 100101, China

[2]University of the Chinese Academy of Sciences, Beijing, China

[3]CAS Key Laboratory of Microbial Physiological and Metabolic Engineering, State Key Laboratory of Transducer Technology, Institute of Microbiology, Chinese Academy of Sciences, Beijing 100101, China

Competing Interest

The authors declare no conflicts of interest in regards to this manuscript.

References

1. Baker SH, Jin S, Aldrich HC, Howard GT, Shively JM (1998) Insertion mutation of the Form I *cbbL* gene encoding ribulose bisphosphate carboxylase/oxygenase (Rubisco) in *Thiobacillus neapolitanus* results in expression of Form II Rubisco, loss of carboxysomes, and an increased CO_2 requirement for growth. J Bacteriol 180(16):4133-4139. https://doi.org/10.1128/JB.180.16.4133-4139.1998
2. Burnap RL, Hagemann M, Kaplan A (2015) Regulation of CO_2 concentrating mechanism in cyanobacteria. Life 5(1):348-371. https://doi.org/10.3390/life5010348
3. Cameron J, Wilson S, Bernstein S, Kerfeld C (2013) Biogenesis of a bacterial organelle: the carboxysome assembly pathway. Cell 155(5):1131-1140. https://doi.org/10.1016/j.cell.2013.10.044
4. Childress JJ, Lee RW, Sanders NK, Felbeck H, Oros DR, Toulmond A, Desbruyeres D, Kennicutt MC, Brooks JJN (1993) Inorganic carbon uptake in hydrothermal vent tubeworms facilitated by high environmental pCO_2. Nature 362(6416):147-149. https://doi.org/10.1038/362147a0
5. Davidi D, Shamshoum M, Guo Z, Bar-On YM, Prywes N, Oz A, Jablonska J, Flamholz A, Wernick DG, Antonovsky N, de Pins B, Shachar L, Hochhauser D, Peleg Y, Albeck S, Sharon I, Mueller-Cajar O, Milo R (2020) Highly active rubiscos discovered by systematic interrogation of natural sequence diversity. EMBO J 39(18):e104081. https://doi.org/10.15252/embj.2019104081

6. Durao P, Aigner H, Nagy P, Mueller-Cajar O, Hartl FU, Hayer-Hartl M (2015) Opposing effects of folding and assembly chaperones on evolvability of Rubisco. Nat Chem Biol 11(2):148-155. https://doi.org/10.1038/nchembio.1715
7. Eisenhut M, Huege J, Schwarz D, Bauwe H, Kopka J, Hagemann M (2008) Metabolome phenotyping of inorganic carbon limitation in cells of the wild type and photorespiratory mutants of the cyanobacterium *Synechocystis* sp. strain PCC 6803. Plant Physiol 148(4):2109-2120. https://doi.org/10.1104/pp.108.129403
8. Eisenhut M, Kahlon S, Hasse D, Ewald R, Lieman-Hurwitz J, Ogawa T, Ruth W, Bauwe H, Kaplan A, Hagemann M (2006) The plant-like C2 glycolate cycle and the bacterial-like glycerate pathway cooperate in phosphoglycolate metabolism in cyanobacteria. Plant Physiol 142(1):333-342. https://doi.org/10.1104/pp.106.082982
9. Eisenhut M, Ruth W, Haimovich M, Bauwe H, Kaplan A, Hagemann M (2008) The photorespiratory glycolate metabolism is essential for cyanobacteria and might have been conveyed endosymbiontically to plants. Proc Natl Acad Sci U S A 105(44):17199-17204. https://doi.org/10.1073/pnas.0807043105
10. Erb TJ, Zarzycki J (2018) A short history of Rubisco: the rise and fall (?) of nature's predominant CO_2 fixing enzyme. Curr Opin Biotechnol 49:100-107. https://doi.org/10.1016/j.copbio.2017.07.017
11. Espie GS, Kimber MS (2011) Carboxysomes: cyanobacterial Rubisco comes in small packages. Photosynth Res 109(1):7-20. https://doi.org/10.1007/s11120-011-9656-y
12. Fernie AR, Bauwe H (2020) Wasteful, essential, evolutionary stepping stone? The multiple personalities of the photorespiratory pathway. Plant J 102(4):666-677. https://doi.org/10.1111/tpj.14669
13. Gao XY, Sun T, Pei GS, Chen L, Zhang WW (2016) Cyanobacterial chassis engineering for enhancing production of biofuels and chemicals. Appl Microbiol Biotechnol 100(8):3401-3413. https://doi.org/10.1007/s00253-016-7374-2
14. Hu GP, Li Y, Ye C, Liu LM, Chen XL (2019) Engineering microorganisms for enhanced CO_2 sequestration. Trends Biotechnol 37(5):532-547. https://doi.org/10.1016/j.tibtech.2018.10.008
15. Jensen RG (2000) Activation of Rubisco regulates photosynthesis at high temperature and CO_2. Proc Natl Acad Sci U S A 97(24):12937-12938. https://doi.org/10.1073/pnas.97.24.12937
16. Lindberg P, Park S, Melis A (2010) Engineering a platform for photosynthetic isoprene production in cyanobacteria, using *Synechocystis* as the model organism. Metab Eng 12(1):70-79. https://doi.org/10.1016/j.ymben.2009.10.001
17. Luan GD, Zhang SS, Lu XF (2020) Engineering cyanobacteria chassis cells toward more efficient photosynthesis. Curr Opin Biotechnol 62:1-6. https://doi.org/10.1016/j.copbio.2019.07.004
18. Lutz RA, Shank TM, Fornari DJ, Haymon RM, Lilley MD, Von Damm KL, Desbruyeres D (1994) Rapid growth at deep-sea vents. Nature 371(6499):663-664. https://doi.org/10.1038/371663a0

19. Mangan NM, Flamholz A, Hood RD, Milo R, Savage DF (2016) pH determines the energetic efficiency of the cyanobacterial CO_2 concentrating mechanism. Proc Natl Acad Sci U S A 113(36):E5354-E5362. https://doi.org/10.1073/pnas.1525145113
20. Moroney JV, Jungnick N, DiMario RJ, Longstreth DJ (2013) Photorespiration and carbon concentrating mechanisms: two adaptations to high O_2, low CO_2 conditions. Photosynth Res 117(1):121-131. https://doi.org/10.1007/s11120-013-9865-7
21. Oliver JWK, Atsumi S (2014) Metabolic design for cyanobacterial chemical synthesis. Photosynth Res 120(3):249-261. https://doi.org/10.1007/s11120-014-9997-4
22. Price GD (2011) Inorganic carbon transporters of the cyanobacterial CO_2 concentrating mechanism. Photosynth Res 109(1-3):47-57. https://doi.org/10.1007/s11120-010-9608-y
23. Price GD, Badger MR, Woodger FJ, Long BM (2008) Advances in understanding the cyanobacterial CO_2-concentrating-mechanism (CCM): functional components, Ci transporters, diversity, genetic regulation and prospects for engineering into plants. J Exp Bot 59(7):1441-1461. https://doi.org/10.1093/jxb/erm112
24. South PF, Cavanagh AP, Lopez-Calcagno PE, Raines CA, Ort DR (2018) Optimizing photorespiration for improved crop productivity. J Integr Plant Biol 60(12):1217-1230. https://doi.org/10.1111/jipb.12709
25. Spreitzer RJ, Salvucci ME (2002) Rubisco: structure, regulatory interactions, and possibilities for a better enzyme. Annu Rev Plant Biol 53(1):449-475. https://doi.org/10.1146/annurev.arplant.53.100301.135233
26. Zahoor A, Otten A, Wendisch VF (2014) Metabolic engineering of *Corynebacterium glutamicum* for glycolate production. J Biotechnol 192:366-375. https://doi.org/10.1016/j.jbiotec.2013.12.020
27. Zhan T, Chen Q, Zhang C, Bi CH, Zhang XL (2020) Constructing a novel biosynthetic pathway for the production of glycolate from glycerol in *Escherichia coli*. ACS Synth Biol 9(9):2600-2609. https://doi.org/10.1021/acssynbio.0c00404

Figures

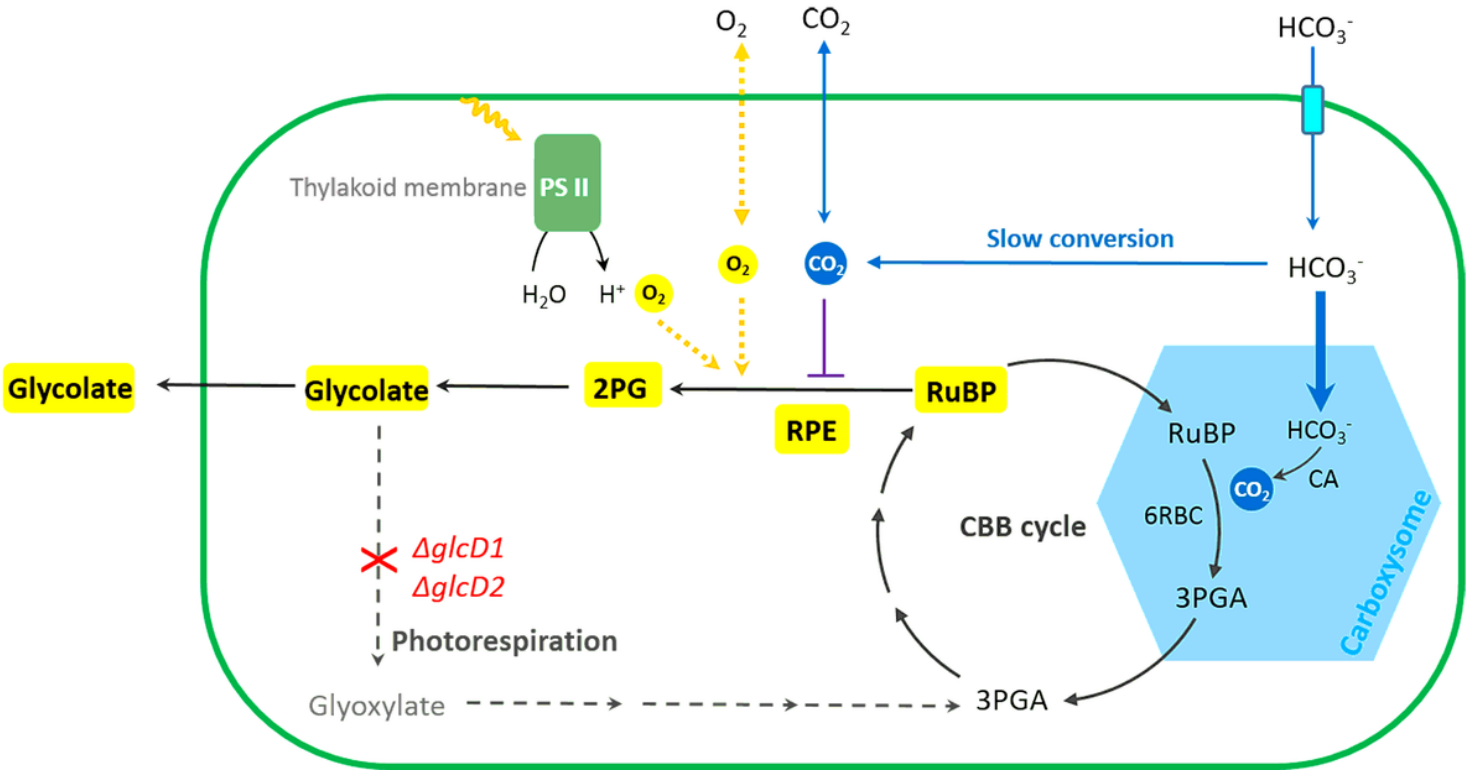

Figure 1

Diagram of glycolate production via oxygenation function of Form II Rubisco in Synechocystis sp. PCC 6803. HCO3- is actively pumped (light blue) into the cytosol. While some of HCO3- spontaneously converts to CO2 in cytosol, most of HCO3- enters the carboxysome (blue hexagons) and is converted to CO2 by the sequestered carbonic anhydrase (CA). RuBP enters the carboxysome and the sequestered Rubisco of Synechocystis (6RBC Rubisco) combines RuBP with CO2 to generated two molecules of 3-phophoglycerate (3PGA). 3PGA escapes to the cytosol and RuBP is regenerated through the Calvin-Benson-Bassham (CBB) cycle. Photorespiration (gray dashed arrows) can be blocked by inactivating (red cross) two glycolate dehydrogenases (GlcD) encoding by glcD1 and glcD2, respectively. The resulting double mutant WT-ΔglcD accumulates and secrets glycolate to the culture (yellow). Form II Rubisco from the endosymbiont of Riftia pachyptila (RPE Rubisco) was overexpressed in strain WT-ΔglcD and located in the cytosol. As cyanobacteria performs oxygenic photosynthesis, RPE Rubisco catalyzes the oxygenation of RuBP to 2-photoglycolate (2PG), facilitating the glycolate production. As CO2 can freely diffuse to the cytosol (blue solid arrow), the elevated CO2 level inhibits the oxygenase function of RPE (purple solid line) and decrease the glycolate production when the external inorganic carbon is supplied with CO2.

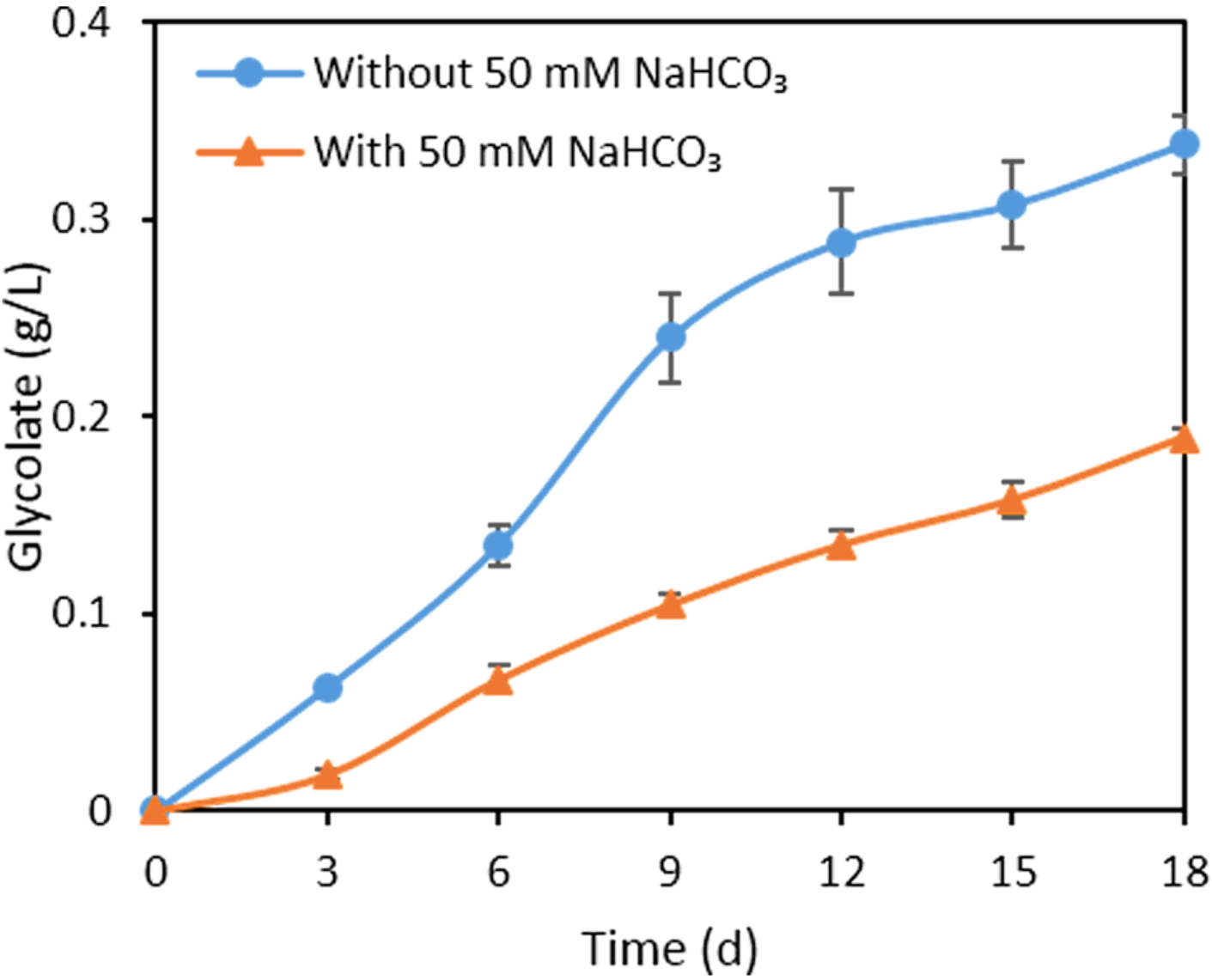

Figure 2

Glycolate production by strain WT-ΔglcD with or without supply of 50 mM NaHCO3. The cells were cultivated at 30oC under 100 µmol protons m-2s-1 light intensity. Error bars represent standard deviations from biological triplicates conducted in three independent experiments.

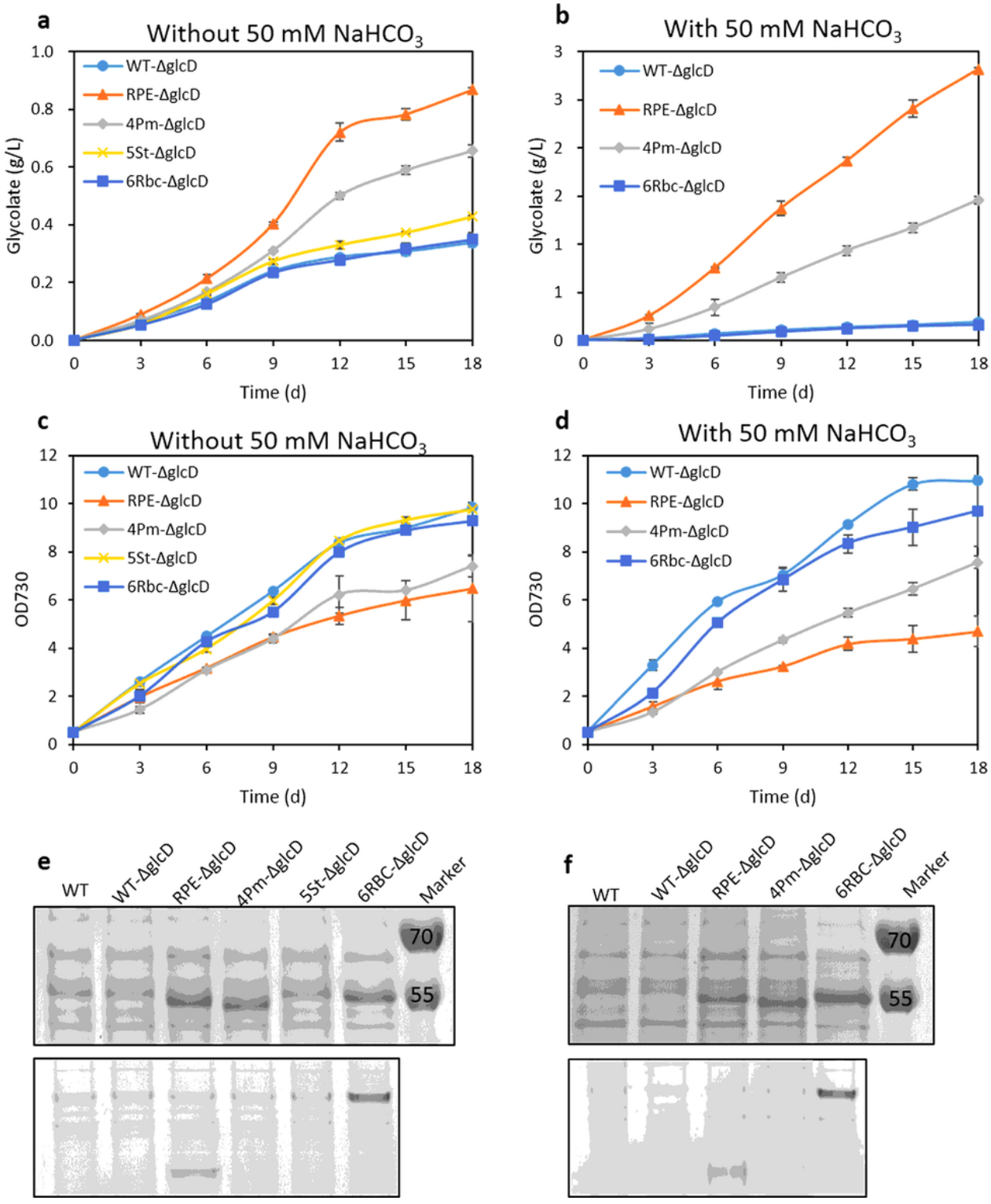

Figure 3

Overexpression of Form II Rubisco increased glycolate production. Glycolate production (A and D), growth curve (B and E) and the protein expression analysis (C and E) of the Synechocystis strains expressing different Form II Rubiscos. The cells were cultivated without or with 50 mM NaHCO3 at 30oC under 100 µmol protons m-2s-1 light intensity. Error bars represent standard deviations from biological triplicates

conducted in three independent experiments. The expression (up) and assembly (down) level of Form II Rubiscos under both conditions were detected with SDS-PAGE and Native-PAGE respectively.

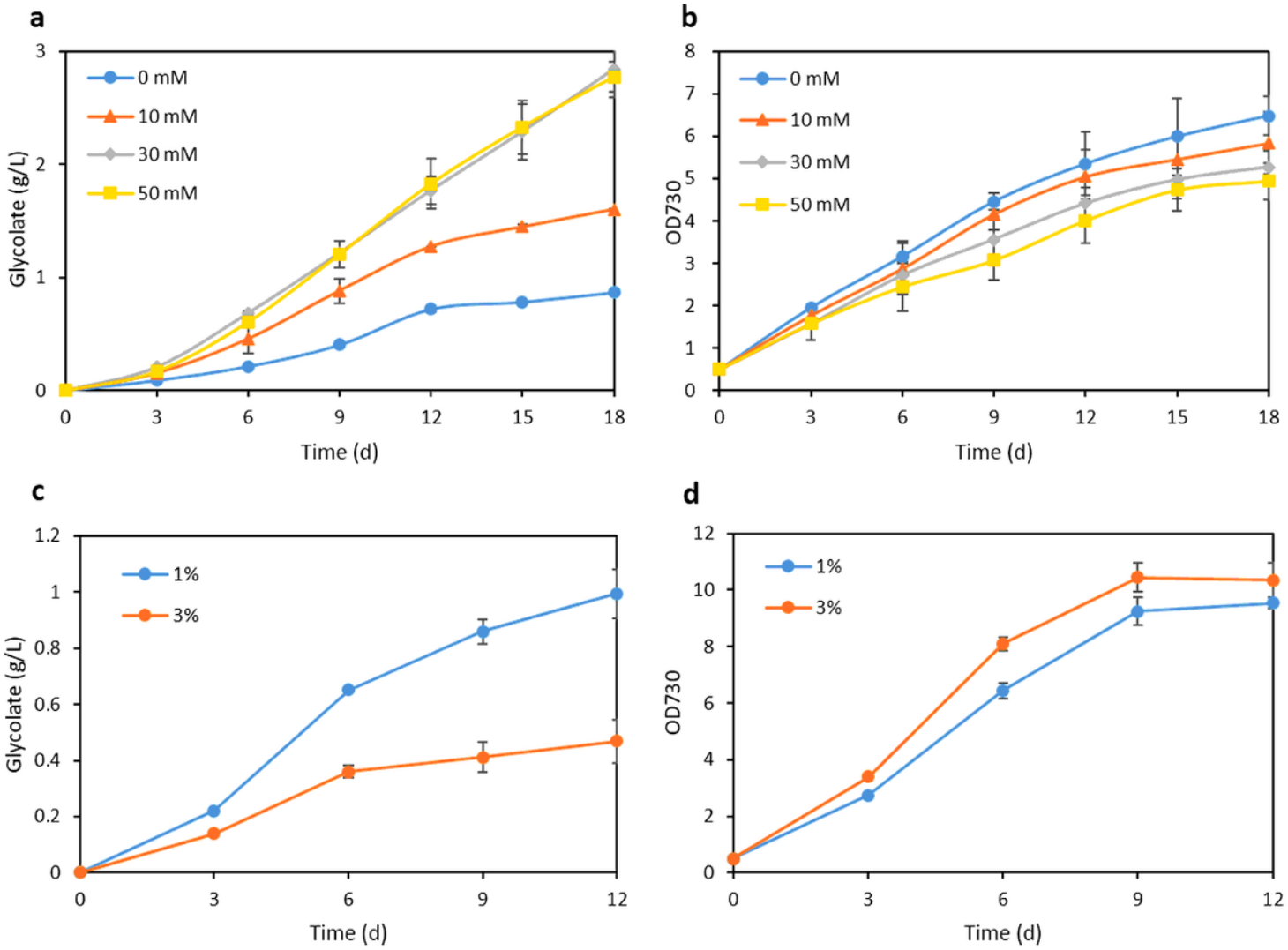

Figure 4

Glycolate production and growth profile of strain RPE-ΔglcD with supply of NaHCO3 or CO2. Cell were cultivated with different concentration of NaHCO3 (A and B) or CO2 (C and D) at 30oC under 100 μmol protons m-2s-1 light intensity. Error bars represent standard deviations from biological triplicates conducted in three independent experiments.

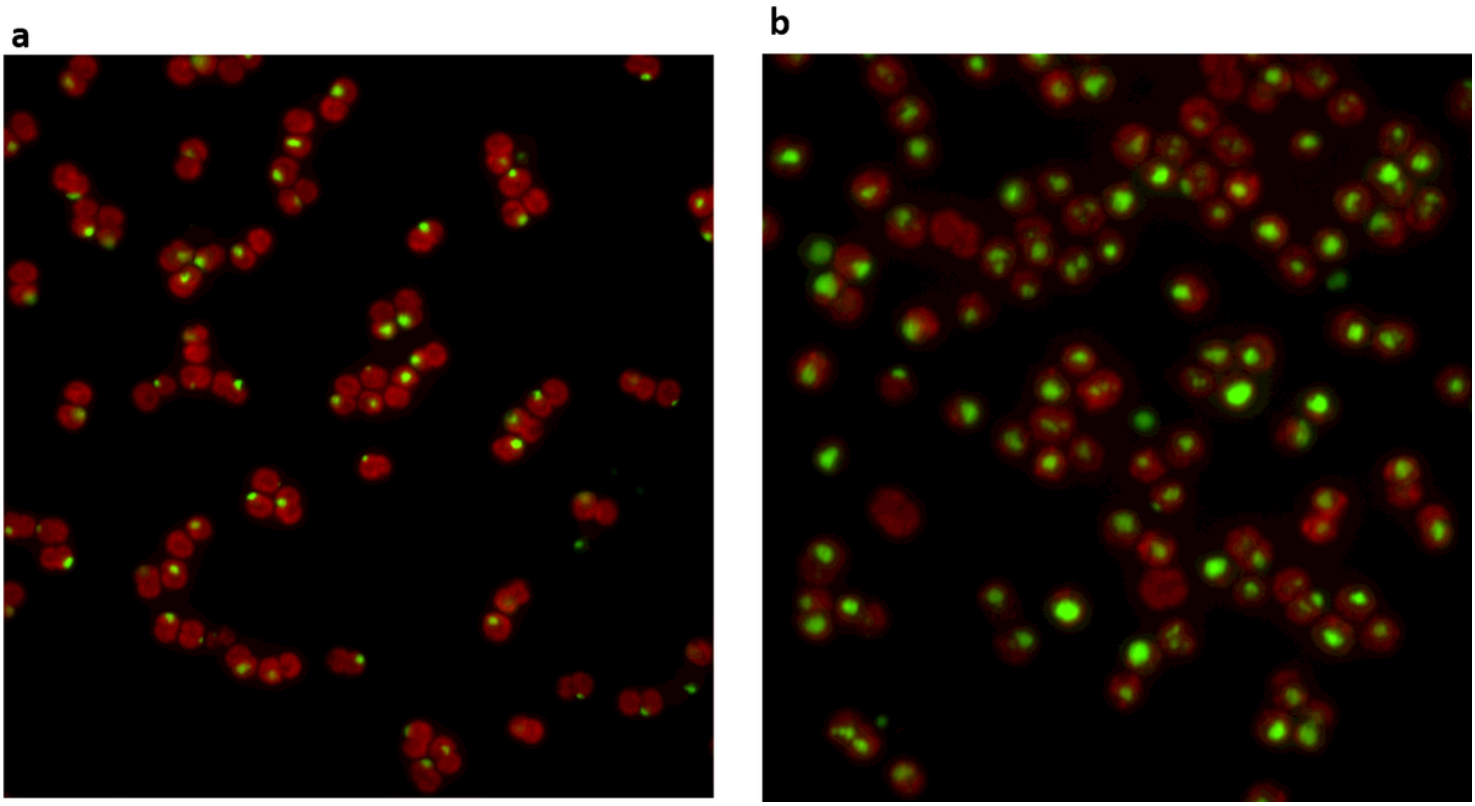

Figure 5

Location of RPE Rubisco in the Synechocystis strain. The fluorescent signal of RPE-GFP (A) and 6RBCL-GFP (B). GFP was fused to the C-terminal of RPE Rubisco or the large subunit of 6RBC Rubisco. RPE-GFP and 6RBCL-GFP was individually expressed in the WT strain. The foci of 6RBC-GFP represents the location of mature carboxysomes. The red fluorescence of endogenous chlorophyll-a was used to indicate the shape of the whole cell.

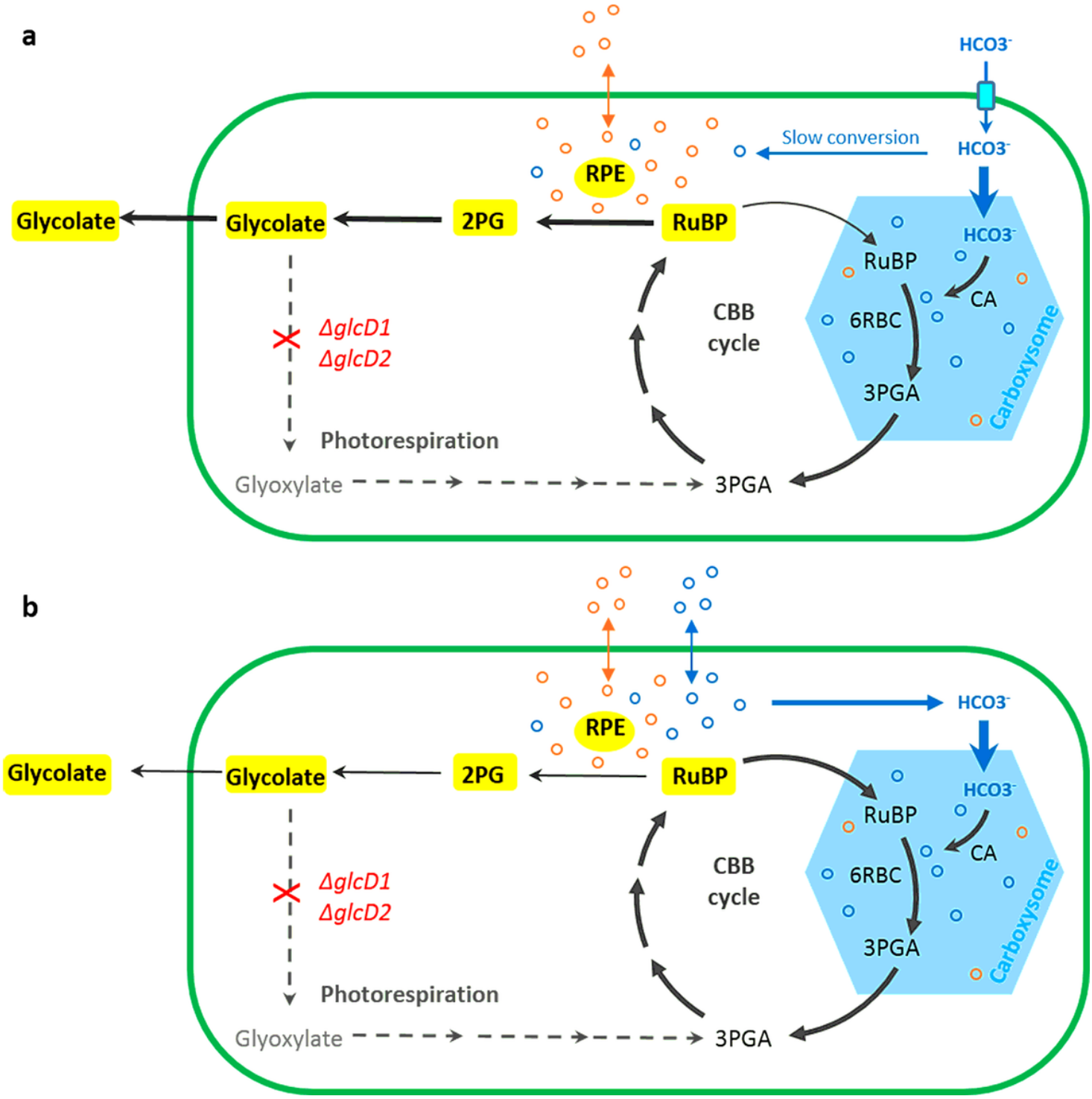

Figure 6

The different impacts of HCO3- (a) and CO2 (b) on glycolate production by RPE-ΔglcD. The orange cycles represent molecule oxygen and the blue cycles represent CO2. The diffusions of O2 and CO2 are indicated by orange and blue double headed-arrows, respectively. Bold solid dark arrows indicate the direction of the favored reaction under the growth conditions.

Supplementary Files

This is a list of supplementary files associated with this preprint. Click to download.

- SupplementalFiles.docx